Available online at www.sciencedirect.com
ScienceDirect
Journal of the European Ceramic Society 30 (2010) 3023–3033
www.elsevier.com/locate/jeurceramsoc

Cure depth for photopolymerization of ceramic suspensions

Vladislava Tomeckova, John W. Halloran *

University of Michigan, Ann Arbor, MI 48109-2136, USA

Received 27 April 2010; accepted 15 June 2010
Available online 24 July 2010

Abstract

The cure depth of a series of photopolymerizable SiO_2 and Al_2O_3 ceramic suspensions was measured as a function of energy dose to determine the sensitivity parameter D_p and its dependence on ceramic volume fraction, type and concentration of photoinitiator and inert dye. As predicted by an Absorption Model for D_p, $1/D_p$ is a linear function of photoinitiator concentration and dye concentration. The molar extinction coefficients derived from the cure depth measurements using an Absorption Model were compared with coefficients determined via spectrophotometry.

Keywords: Photopolymerization; SiO_2; Al_2O_3; Suspensions

1. Introduction

Photopolymerizable suspensions have been used in a dental resins,[1] patterned substrates[2] and layered manufacturing of ceramics[3,4] by techniques such as stereolithography.

Photopolymerizable suspensions consist of ceramic particles dispersed in liquid monomers with photoinitiators (PIs) as the photoactive substances that initiate the polymerization reactions upon illumination. The polymerization behavior is affected by the type and concentration of photoinitiators, and the fundamental kinetic parameters of the monomer. The behavior can be modified with inert dyes that absorb photons without creating free radicals and inhibitors that destroy free radicals. Scattering of the UV due to the index of refraction contrast between the ceramic particles and the monomer also affects photopolymerization.

A dose of UV of energy E will cause polymerization to a depth C_d as described by the Jacob's equation[5] as $C_d = D_p \ln(E/E_c)$, where E_c is the critical energy and D_p is the sensitivity of the photopolymerizable suspension. Recently, we proposed simple predictive models for the photosensitivity in terms of absorption of UV photons and critical energy in terms of exhaustion of inhibitors.[6] The Inhibitor Exhaustion Model for E_c is discussed in another paper.[7] This paper concerns the Absorption Model for the sensitivity term D_p and compares some detailed data with predictions of the model. The Absorption Model[6] considers the attenuation of the UV beam by absorption from dyes and photoinitiators, and by scattering of the UV by particles. These are related by:

$$\frac{1}{D_p} = S + A - \Phi A \tag{1}$$

where S is the scattering term reporting the effects of light scattering and A is the absorption parameter reporting the effect of the active photoinitiators (PIs) and inert dyes for suspensions containing ceramic at a volume fraction ϕ. The scattering parameter is defined as $S = 1/l_{sc}$ (reciprocal scattering length l_{sc}) and the absorption parameter is related to the properties of the PI and dye as $A = (\varepsilon_P c_P + \varepsilon_D c_D)$, where c_P is the concentration of the PI in mol/unit volume and ε_P is molar extinction coefficients in L/(mol cm) of the PI. Similar terms for the inert dye is the dye concentration c_D and the dye molar extinction coefficient ε_D. Eq. (1) can be written as:

$$\frac{1}{D_p} = S + (1 - \Phi)(\varepsilon_P c_P + \varepsilon_D c_D) \tag{2}$$

The Absorption Model predicts that $1/D_p$ plotted against c_P should be a straight line. The slope of the line K_3 depends on

* Corresponding author at: Department of Materials Science and Engineering, University of Michigan, 2300 Hayward Street, Ann Arbor, MI 48109-2136, USA. Tel.: +1 734 763 1051; fax: +1 734 763 4788.
E-mail address: peterjon@umich.edu (J.W. Halloran).

0955-2219/$ – see front matter © 2010 Elsevier Ltd. All rights reserved.
doi:10.1016/j.jeurceramsoc.2010.06.004

photoinitiator molar extinction coefficient as shown in Eq. (3a):

$$\frac{d(1/D_p)}{dc_P} = K_3 = (1-\Phi)\varepsilon_P \tag{3a}$$

The intercept of the straight line I_3 involves the scattering term and the dye concentration and molar extinction coefficient as shown in Eq. (3b):

$$\left(\frac{1}{D_p}\right)_{\text{for} c_P=0} = I_3 = S + (1-\Phi)\varepsilon_D c_D \tag{3b}$$

Note that the scattering term depends on the refractive index[8,9] and volume fraction[9,10] of the ceramic, as discussed in more detail in the previous paper.[6] The slope K_3 should be larger for compositions with less ceramic volume content. The molar extinction coefficient can be calculated from the slope. The intercept I_3 provides the information about two parameters, the scattering term S and the dye term. For compositions with no dye ($c_D = 0$), the scattering term can be directly determined. The intercept should increase with decreasing ceramic volume content and with increasing dye concentration.

The model also predicts that $1/D_p$ vs. c_D is a straight line. The slope K_4 depends on the absorption coefficient of the dye as in Eq. (4a):

$$\frac{d(1/D_p)}{dc_D} = K_4 = (1-\Phi)\varepsilon_D \tag{4a}$$

The intercept of the $1/D_p$ vs. dye concentration line I_4 gives another estimate of the scattering term S and the PI molar absorption coefficient.

$$\left(\frac{1}{D_p}\right)_{\text{for} c_D=0} = I_4 = S + (1-\Phi)\varepsilon_P c_P \tag{4b}$$

The slope of the dye concentration line should increase with decreasing ceramic volume content. The slope reports on the molar extinction coefficient of the dye. The intercept should increase with decreasing ceramic volume concentration and increasing PI concentration. Two sets of experiments, with D_p as a function of dye concentration and as a function of PI concentration, provides two independent estimates for the parameters in the Absorption Model. The molar extinction coefficients from the cure depth measurements can be compared with values measured by spectrophotometry.

This work explores the validity of the Absorption Model for about 100 suspensions with varying ceramic volume content, photoinitiator type and concentration, the presence of UV and visible light absorber, inhibitor and light stabilizers. Most of the suspensions were prepared with silica, with more limited data for alumina suspensions. Polymerization is conducted with a 355 nm UV laser and with mercury vapor UV lamps.

2. Experimental procedure

2.1. Materials

Details of the photopolymerizable suspensions are presented elsewhere.[5] Briefly, the photocurable monomer system is consists of 87.5 wt% of the bifunctional monomer 1,6-hexanediol diacrylate (SR238, Sartomer, USA) and 12.5 wt% of the tetrafunctional monomer ethoxylated pentaerythritol tetraacrylate (SR494, Sartomer, USA). Both are low viscosity fast curing acrylates. These monomers are transparent to UV for wavelengths longer than about 320 nm. The photoinitiator for most of the experiments was a non-photobleaching ketone 1-hydroxy-cyclohexyl-phenyl-ketone (Irgaure 184, Ciba, USA). A limited number of experiments were conduced with a photobleaching phosphine oxide, phenylbis(2,4,6-trimethyl benzoyl) (Irgacure 819, Ciba, USA). The inert UV absorbing dye was from the hydroxyphenylbenzotriazole class with main component phenol, 2-(2H-benzotriazol-2-yl)-6-dodecyl-4-methyl-, branched and linear (Tinuvin 171 (Ciba, USA)). Some experiments were done with a "blue light absorber" 3H-Pyrazol-3-one, 4-[(1,5-dihydro-3-methyl-5-oxo-1-phenyl-4Hpyrazol-4-ylidene)methyl]-2,4-dihydro-5-methyl-2-phenyl thermoplast yellow 104 (BASF, USA). The effect of inhibitors was studied using one inhibitor 2-methoxyhydroquinone, 98% (Sigma–Aldrich, USA) and one hindered amine light stabilizer (HALS) Tinuvin 123 (Ciba, USA). An overview of photoinitiators, dyes, radical scavengers and inhibitors is also summarized in Table 1.

Most of the experiments were done with a fused silica powder silicon (IV) oxide, 99.8%, metal basis (Alfa Aesar, USA) with mean diameter 7.1 μm and specific area of 5 m^2/g and density 2.2 g/cm^3 (all from the manufacturer's specifications). Others were done with alumina powder (A16-SG, Alcoa, USA) with particles mean diameter $d_{50} = 0.4$ μm, specific surface area 8.6 m^2/g and density 3.92 g/cm^3 (from the manufacturer's specifications). The colloidal dispersant was an alkoxylated ammonium phosphate Variquat CC-59 (Evonik, Degussa) at the concentration of 2.083% (wrt powder mass). The ceramic suspensions were prepared by ball milling, as described elsewhere.[6]

2.2. Methods

Spectrophotometry was used to determine the molar extinction coefficients of the PIs and light absorbers. PIs and light absorbers were first dissolved in isopropanol in small concentrations. The absorbance of the liquid solution was measured in the wavelength range 300–440 nm using a UV–Vis spectrophotometer (Cary 50 Bio, Varian, Palo Alto, CA, USA). Absorbance was measured at room temperature and the optical path was 1 cm. Molar extinction coefficient ε was calculated using Lambert–Beer law $\varepsilon = A_o/cl$, where A_o is the absorbance, c is the concentration of the photoinitiator or light absorber in mol/L and l is the optical path length. The extinction coefficients are reported for dilute solutions in isopropanol. A limited series of measurements were done with dilute solution in the HDDA monomer, yielded the same values for extinction coefficient.

Cure depth measurements were performed using SLA-250 (3D systems, Inc.). The laser is a solid state laser (Xcyte, JDSU, Milpitas, CA), that has a quasi-continuous wave emitting at 355 nm, output power 30 mW, and a beam diameter of 125 μm. A "wedgeplots" technique was used to determine the sensitivity D_p and critical energy E_c. During the experiment, the laser draws six

Table 1
Properties of used photoinitiators, dyes, radical scavengers and inhibitors (all from manufacturers' specifications).

	Commercial name	Density (g/cm^3)	Molecular weight (g/mol)
Ketone photoinitiator	Irgacure 184	1.1–1.2	204.3
Phosphine oxide photoinitiator	Irgacure 819	1.205	418.5
Triazole dye (UV light absorber)	Tinuvin 171	1.003	~395
Blue light absorber (visible light absorber)	Thermoplast yellow 104	1.3	358.5
Liquid yellow HALS	Tinuvin 123	0.97	737
Inhibitor	Methoxy hydroquinone	–	140.14

Table 2
Absorbance and molar extinction coefficients at 355 nm for ketone PI and triazole dye in isopropanol measured via spectrophotometry.

	Weight concentration [%]	c [mol/L]	A_{355}	ε_p [L/(mol cm)]	ε_P [L/(mol cm)]
Ketone PI	0.1	0.0039	0.1869	48	49 ± 1
	0.08	0.003	0.1513	49	
	0.06	0.0022	0.1159	51	
	0.04	0.0015	0.0763	49	
Triazole dye	0.001	2.01E−05	0.2679	13,300	$13{,}600 \pm 600$
	0.0008	1.58E−05	0.2228	14,100	
	0.0006	1.19E−05	0.1676	14,100	
	0.0004	7.90E−06	0.1018	12,800	

squares exposed to different energy doses, thus resulting in different thicknesses. Polymerized "wedgeplots" were rinsed with isopropanol and the thickness was measured with a micrometer. The cure depths plotted against energy dose is a linear curve with the slope representing the D_p and the energy dose-intercept representing the critical energy, the energy required to initiate the polymerization. The "wedgeplots" technique and the calculations of the errors of the D_p and E_c are discussed in detail in a companion paper.[7]

Some cure depth measurements were performed with a UV system equipped with mercury lamps (Hanovia, Newark NJ USA). The mercury lamps have strong lines at 305, 315, 365, 405 and 435 nm. Cure depth measurements were performed with 300 W lamps. Light exposure was calibrated using a radiometer (UV-integrator PC-2008, Hanovia, Newark, NJ, USA).

3. Results and discussion

3.1. Spectrophotometry

Absorbance curves of the ketone and phosphine oxide PIs and light absorbers (the triazole dye and blue light absorber) in the wavelength range 300–440 nm are shown in Fig. 1. The molar extinction coefficients of the ketone PI and the triazole dye at 355 nm were determined to be 49 ± 1 L/(mol cm) and $13{,}600 \pm 600$ L/(mol cm), respectively. The more detailed absorbance data at 355 nm for the ketone PI and the triazole dye at 4 different concentrations appear in Table 2.

To determine the molar extinction coefficients at multiple wavelengths for the mercury lamps, the absorbance has to be convoluted considering the portions of the light absorbed at individual wavelengths. The mercury vapor lamp had with 5 lines at 305 nm (10% relative intensity), 315 nm (16%), 365 nm (30%), 405 nm (11%) and 435 nm (33%). The absorption spectrum for the example of 0.1 wt% ketone PI (in isopropanol) has absorbance of 0.770 at 305 nm, 0.428 at 315 nm, 0.077 at 365 nm, with no absorbance at the 405 and 435 nm lines. The $A_{convoluted}$ for this example is $0.770(0.10) + 0.428(0.16) + 0.077(0.30) + 0 + 0 = 0.169$. The convoluted molar extinction coefficient was then calculated to be $\varepsilon_{P,convoluted} = 44$ L/(mol cm) for this case. The average convoluted molar extinction coefficients at multiple mercury lamp wavelengths are 40 ± 2 L/(mol cm) for the ketone PI, 2500 ± 30 L/(mol cm) for the photobleaching phosphine oxide PI and $13{,}100 \pm 1900$ L/(mol cm) for the blue light absorbing dye. Note that the light absorbers (dyes) are generally much stronger absorbers than the PIs. The more detailed data for the ketone and phosphine oxide PIs and the blue light absorber

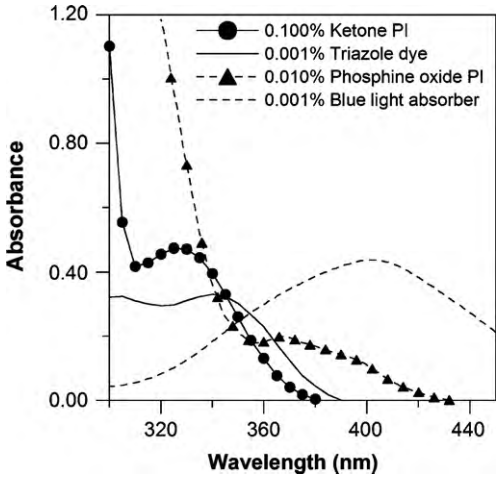

Fig. 1. Absorbance vs. wavelength for ketone and phosphine oxide photoinitiators and UV light absorber (triazole dye) and visible light absorber (blue light absorber). Substances were dissolved in isopropanol and the optical path was 1 cm. The concentration of the substances is expressed as wt% in isopropanol.

Table 3
Absorbance and molar extinction coefficients at multiple Hanovia wavelengths for ketone and phosphine oxide PIs and blue light absorber in isopropanol. The convolution theory was used to determine molar extinction coefficients over multiple wavelengths.

	Wt%	c [mol/L]	A_{305} (10%)	A_{315} (16%)	A_{365} (30%)	A_{405} (11%)	A_{435} (33%)	$A_{convoluted}$	$\varepsilon_{P,convoluted}$ [L/(mol cm)]	$\varepsilon_{P,convoluted}$ [L/(mol cm)]
Ketone PI	0.1	0.0039	0.77	0.428	0.077	0	0	0.169	44	40 ± 2
	0.08	0.003	0.456	0.336	0.063	0	0	0.119	39	
	0.06	0.0022	0.337	0.25	0.049	0	0	0.089	39	
	0.04	0.0015	0.23	0.172	0.031	0	0	0.06	39	
Phosphine oxide PI	0.01	1.83E−04	1.6	1.36	0.197	0.083	0	0.449	2500	2500 ± 30
	0.008	1.50E−04	1.31	1.108	0.15	0.057	0	0.3624	2400	
	0.006	1.13E−04	1	0.86	0.122	0.048	0	0.282	2500	
	0.004	7.60E−05	0.674	0.577	0.079	0.026	0	0.188	2500	
Blue light absorber	0.001	2.19E−05	0.047	0.068	0.325	0.437	0.302	0.261	12,500	$13{,}100 \pm 1900$
	0.0006	1.31E−05	0.037	0.049	0.192	0.253	0.188	0.159	12,100	
	0.0004	8.90E−06	0.054	0.061	0.164	0.206	0.167	0.142	15,900	
	0.0002	4.50E−06	0.016	0.02	0.072	0.09	0.059	0.056	11,900	

at lamp multiple wavelengths appear in Table 3 for different concentrations of PIs and the dye.

3.2. Cure depth vs. energy dose

Shown in Fig. 2 is the raw cure depth data vs. energy for 60 vol% SiO_2 suspensions with an inhibitor MEHQ and the liquid yellow HALS. The HALSs behave similarly as inhibitors, since they scavenge free radicals. The suspensions contain the ketone PI (0.1008 mol/L wrt monomer). According to Jacob's equation, the slope of the curves represents the sensitivity D_p and the x-intercept represents the critical energy E_c. Notice that the addition of the MEHQ resulted in a series of almost parallel curves when the D_p varied from ~600 to 470 μm. Similarly, the presence of the liquid yellow HALS did not have almost any impact on the sensitivity since the D_p varied from ~600 to ~550 μm. The Absorption Model predicts that sensitivity (the slopes of the lines in Fig. 2) should not be affected by inhibitors and this is confirmed over a range of compositions.

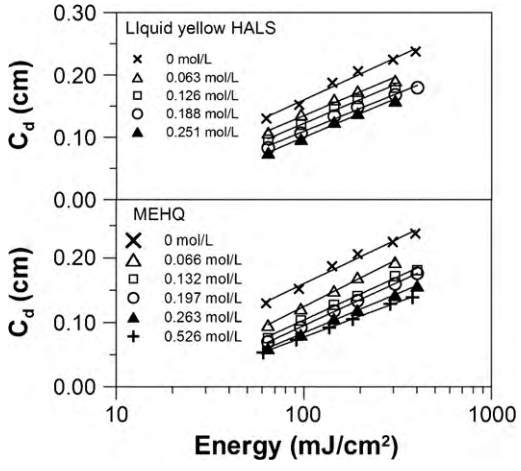

Fig. 2. Cure depths vs. energy dose for 60 vol% SiO_2 suspension with ketone PI (0.1008 mol/L wrt monomer). Compositions contained inhibitor MEHQ or the liquid yellow HALS. Cure depth measurements were performed using the 355 nm laser.

Increasing the inhibitor concentration should increase the critical energy (the intercept in Fig. 2). The effect of the inhibitor and HALS on the critical energy increase is discussed in a companion paper.[7]

3.3. Effect of photoinitiator concentration on sensitivity

The Absorption Model predicts that $1/D_p$ plotted against c_P is a straight line and the slope should increase with decreasing ceramic volume content, as in Eq. (3a). For compositions with no dye, the intercept is equal to the scattering term S. This prediction was tested on a series of suspensions with the non-photobleaching ketone PI.

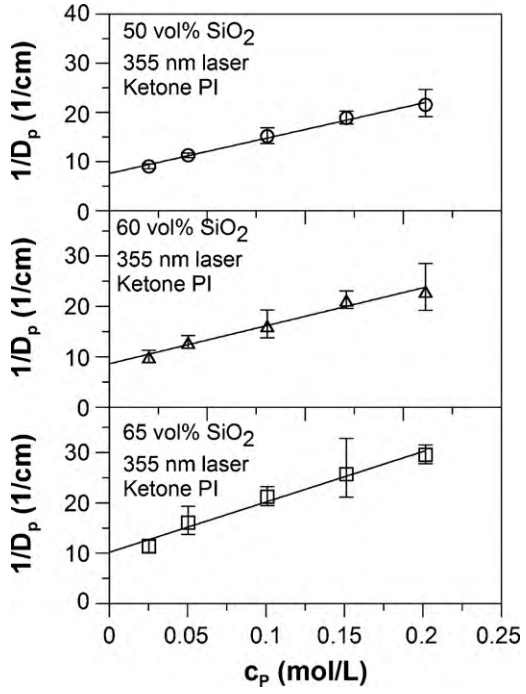

Fig. 3. $1/D_p$ vs. photoinitiator concentration c_P for SiO_2 suspensions with ketone PI. The suspensions contain no dye ($c_D = 0$). Cure depth measurements were performed using the 355 nm laser.

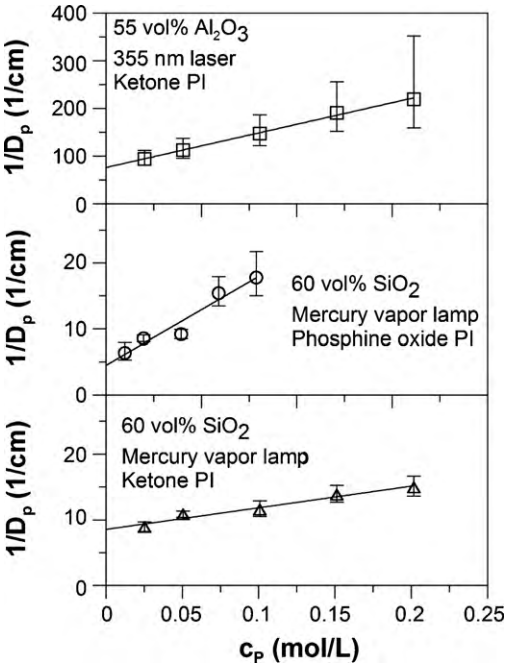

Fig. 4. $1/D_p$ vs. photoinitiator concentration c_P for SiO_2 and Al_2O_3 suspensions. The suspensions contain no dye ($c_D = 0$). Cure depth measurements were performed using the 355 nm laser and vapor mercury lamp.

Fig. 3 shows the $1/D_p$ vs. c_P for 50, 60 and 65 vol% SiO_2 suspensions with ketone PI polymerized using the 355 nm laser. Fig. 4 shows $1/D_p$ data for 55 vol% Al_2O_3 suspensions polymerized using the 355 nm laser. Fig. 4 also has $1/D_p$ data for 60 vol% SiO_2 suspensions polymerized using the mercury vapor lamp with ketone PI and photobleaching phosphine PI. For all these cases, $1/D_p$ is indeed a linear function of the concentration of photoinitiator, as predicted by the Absorption Model. The values of the slopes, intercepts and correlation coefficients of the regression lines are summarized in Table 4. Since these suspensions contain no dye ($c_D = 0$), the situation is simplified. The intercept I_3 can be used to directly determine the scattering term S and molar extinction coefficient of the photoinitiator can be determined from the slopes K_3.

For suspensions with ketone PI cured with the 355 nm laser, the scattering term S was determined to be $\sim 7.2 \pm 0.5\ cm^{-1}$ for 50 vol% SiO_2 suspension, $8.1 \pm 1.4\ cm^{-1}$ for 60 vol% SiO_2 suspensions and $9.4 \pm 0.9\ cm^{-1}$ for 65 vol% SiO_2 suspension. For the scattering term S of 60 vol% SiO_2 suspensions polymerized using the mercury vapor lamp was determined to be $8.8 \pm 0.7\ cm^{-1}$ for suspension with the ketone PI. This is close to the S value for the 60% silica suspension cured with the laser. This is expected from the Absorption Model. However, for the 60% silica suspension with the phosphine PI, the intercept gave a scattering term value of $S = 6.0 \pm 1.0\ cm^{-1}$, which is somewhat smaller.

The Al_2O_3 suspensions exhibited a significantly larger scattering term of $75.5 \pm 22.3\ cm^{-1}$, which is ~10 times higher than the scattering terms of silica suspensions. This is to be expected, since the alumina has a higher refractive index and smaller particle size, and so has more potent scattering.[8–11]

The values for the molar extinction coefficient of the ketone PI, obtained using Eq. (3a) from the cure depth measurements of silica suspensions using the 355 nm laser, varied from 150 L/(mol cm) for 50% suspensions to 300 L/(mol cm) for 65% suspensions, with an average of 220 L/(mol cm). These are approximately in the same range, but from the Absorption Model we expect the value of the extinction coefficient to be insensitive to the ceramic loading. The convoluted ketone PI molar absorption coefficient determined from cure depth measurements using the mercury vapor lamp was 80 ± 20 L/(mol cm). This is similar in magnitude, but smaller than the extinction coefficient from the laser curing series.

The Absorption Model values should be compared with the molar extinction coefficient of the ketone PI measured independently via spectrophotometry. The spectrophotometric value was 49 ± 1 L/(mol cm) at 355 nm for the laser and the convoluted extinction coefficient for the multiple wavelengths of the mercury lamp was 40 ± 2 L/(mol cm). The spectrophotometer values are noticeably smaller, but are the same order of magnitude. Considering that two quite different techniques were involved, it is perhaps a satisfactory match. However, the molar extinction coefficient of the ketone PI determined from Al_2O_3 suspensions was $\sim 1600 \pm 800$ L/(mol cm), which is much higher than those determined from silica suspensions and via spectrophotometry. This is unexpected, since the Absorption Model predicts that extinction coefficients from the slope would be the same. The scattering is much stronger with the alumina suspensions, but this should not affect the slope term, if the Absorption Model is correct. Perhaps the treatment of scattering and absorption in the Model is not quite accurate, so that the apparent extinction coefficients are overestimated in a scattering-dominant case.

For silica suspensions with the photobleaching phosphine oxide PI, the molar extinction coefficient inferred from cure

Table 4
Slopes and intercept determined from $1/D_p$ vs. c_P for SiO_2 and Al_2O_3 suspensions with no dye.

Light source	Ceramic	ϕ	PI	r^2	K_3	$I_3 = S$ [1/cm]	ε_P [L/(mol cm)]
355 nm laser	SiO_2	0.5	Ketone	0.99	77 ± 9	7.2 ± 0.5	150 ± 20
		0.6	Ketone	0.98	84 ± 16	8.1 ± 1.4	210 ± 40
		0.65	Ketone	0.98	103 ± 8	9.4 ± 0.9	300 ± 20
Average							220
Mercury vapor lamp	SiO_2	0.6	Ketone	0.87	33 ± 8	8.8 ± 0.7	80 ± 20
			Phosphine oxide	0.55	84 ± 26	6.0 ± 1.0	210 ± 70
355 nm laser	Al_2O_3	0.55	Ketone	1	734 ± 370	75.5 ± 22.3	1600 ± 800

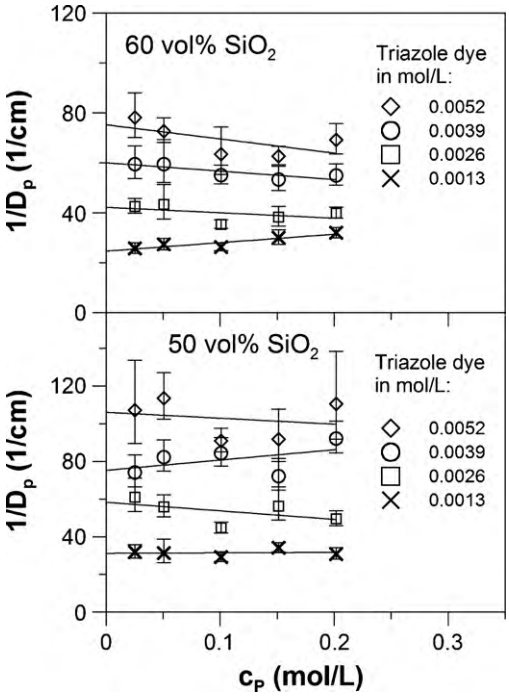

Fig. 5. $1/D_p$ vs. photoinitiator concentration c_P for 50 and 60 vol% SiO_2 suspensions with ketone PI and triazole dye. Cure depth measurements were performed using the 355 nm laser.

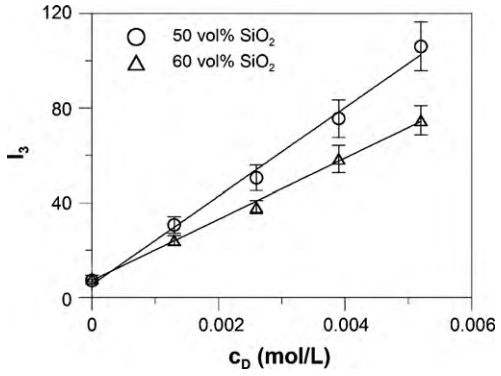

Fig. 6. I_3 vs. c_D for 50 and 60 vol% SiO_2 suspensions with ketone PI and triazole dye. Cure depth measurements were performed using the 355 nm laser.

depth measurements using Eq. (3a) was 210 ± 70 L/(mol cm). This is much smaller than the value of 2500 ± 30 L/(mol cm) determined via spectrophotometry. Phosphine oxide is a photobleaching PI, so its effective extinction coefficient decreases upon illumination. The Absorption Model is not strictly applicable, since ε_P is not constant. Thus a value for extinction coefficient inferred from deep curing will underestimate the value from spectrophotometry, where the low intensity does not cause photobleaching. However, for the purpose of estimating cure depth, the value extracted from Eq. (3a) for the bleached condition is probably more useful than the spectrophotometric value in the unbleached condition.

For compositions with inert dye, $1/D_p$ vs. PI concentration c_P should be a straight line, which we observe in Fig. 5 for 50 and 60 vol% silica. The slope K_3 should only depend upon the molar extinction coefficient of the PI, according to the model Eqs. (3a) and (3b) but we can see from Fig. 5 that this is not what we observe. Rather the slope is very small, as if $1/D_p$ is not affected by the concentration of photoinitiator. The data parameters of the regression lines are summarized in Table 5. From these data we can extract a value of the molar extinction coefficient of the triazole dye of $\varepsilon_D \sim 33{,}400$ L/(mol cm). Contrary with what we anticipate with the simple model, the presence or the strongly absorbing triazole dye is making D_p nearly independent of additional PI. Perhaps this is because the extinction coefficient of the PI is only $\varepsilon_P \sim 49$ L/(mol cm). In some cases the slope K_3 of the Fig. 5 lines is actually negative, because the lightly-absorbing PI is diluting the heavily absorbing dye. The model predicts that the intercept I_3 should increase linearly with dye concentration. This is the case, as shown in Fig. 6, a plot of I_3 vs. c_D for both suspensions. The slope of Fig. 6 gives another estimate for the molar extinction coefficient of the triazole dye. Respectively for the 50 and 60 vol% silica suspension, the slope suggests $\varepsilon_D \sim 37{,}300$ L/(mol cm) and $\varepsilon_D \sim 32{,}200$ L/(mol cm), which is similar to the Table 5 values.

3.4. Effect of inert dye concentration on sensitivity

The inverse of the sensitivity is shown as a function of inert triazole dye concentration in Fig. 7 (for 50% silica), Fig. 8 (for 60% silica), and Fig. 9 (for 65% silica), all for several PI concentrations. Fig. 10 presents data for alumina with the ketone PI and silica with the phosphine oxide PI. The Absorption Model predicts that $1/D_p$ vs. c_D should be a straight line, which is observed in all cases. The regression lines are in Table 6a. The slopes K_4

Table 5
Slopes and intercepts of linear regressions $1/D_p$ vs. c_P for 50 and 60 vol% SiO_2 suspensions with ketone PI and triazole dye. Cure depth measurements were performed using the 355 nm laser.

Light source	Ceramic	ϕ	PI	c_D [mol/L]	r^2	K_3	I_3	ε_P [L/(mol cm)]	ε_D [L/(mol cm)]
355 nm laser	SiO_2	0.5	Ketone	0.0013	−0.28	7.2 ± 26.2	30.7 ± 3.6	14.3 ± 52.3	$36{,}100 \pm 4200$
				0.0026	−0.29	-15.5 ± 40.2	50.6 ± 5.3	-31.1 ± 80.5	$33{,}400 \pm 3500$
				0.0039	−0.03	54.1 ± 64.4	75.6 ± 7.9	108.2 ± 128.9	$35{,}000 \pm 3700$
				0.0052	−0.27	-31.4 ± 83.3	106.1 ± 10.3	-62.8 ± 166.7	$38{,}000 \pm 3700$
		0.6	Ketone	0.0013	0.73	34.6 ± 16	24.2 ± 1.9	86.6 ± 40	$31{,}000 \pm 2500$
				0.0026	−0.33	-1.4 ± 20.4	38.3 ± 2.7	-3.4 ± 51.1	$29{,}000 \pm 2100$
				0.0039	0.35	-24.2 ± 41.4	58.5 ± 5.8	-60.5 ± 103.4	$32{,}300 \pm 3200$
				0.0052	0.28	-60.2 ± 45.5	74.8 ± 6.2	-150.5 ± 113.8	$32{,}000 \pm 2600$
Average									33,400

Table 6a
Slopes and intercepts of linear regressions $1/D_p$ vs. c_D for 50, 60 and 65 vol% SiO_2 suspensions with varying ketone PI concentration. Cure depth measurements were performed using the 355 nm laser.

Light source	Ceramic	ϕ	PI	c_P [mol/L]	Dye	r^2	K_4	I_4	ε_D [L/(mol cm)]	ε_P [L/(mol cm)]
355 nm laser	SiO_2	0.5	Ketone	0.0252	Triazole	0.99	17,700 ± 1600	9.0 ± 0.5	35,300 ± 3300	143 ± 8
				0.0504		0.99	18,100 ± 1400	11.2 ± 0.5	36,100 ± 2800	160 ± 7
				0.1008		0.95	13,600 ± 950	13.8 ± 1.6	27,200 ± 1900	132 ± 15
				0.1512		0.99	13,100 ± 1400	18.6 ± 1.3	26,200 ± 2900	151 ± 11
				0.2016		0.83	13,600 ± 1700	18.0 ± 2.8	27,100 ± 3300	107 ± 17
		0.6		0.0252		1	12,600 ± 200	9.7 ± 0.3	31,600 ± 500	163 ± 5
				0.0504		1	11,500 ± 900	12.7 ± 1.3	28,800 ± 2300	228 ± 24
				0.1008		0.93	8800 ± 1000	14.5 ± 2.2	22,100 ± 2500	158 ± 24
				0.1512		0.99	7900 ± 750	20.7 ± 1.7	19,700 ± 1900	208 ± 17
				0.2016		0.95	8397 ± 1200	20.3 ± 2.9	21,000 ± 3000	152 ± 22
		0.65		0.1008		0.89	8000 ± 1100	19.1 ± 1.7	22,700 ± 3300	274 ± 24
				0.1512		0.92	8800 ± 1250	20.0 ± 3.5	25,100 ± 3600	200 ± 35
				0.2016		0.83	6900 ± 800	26.6 ± 1.8	19,600 ± 2300	243 ± 16
Average									26,400	180

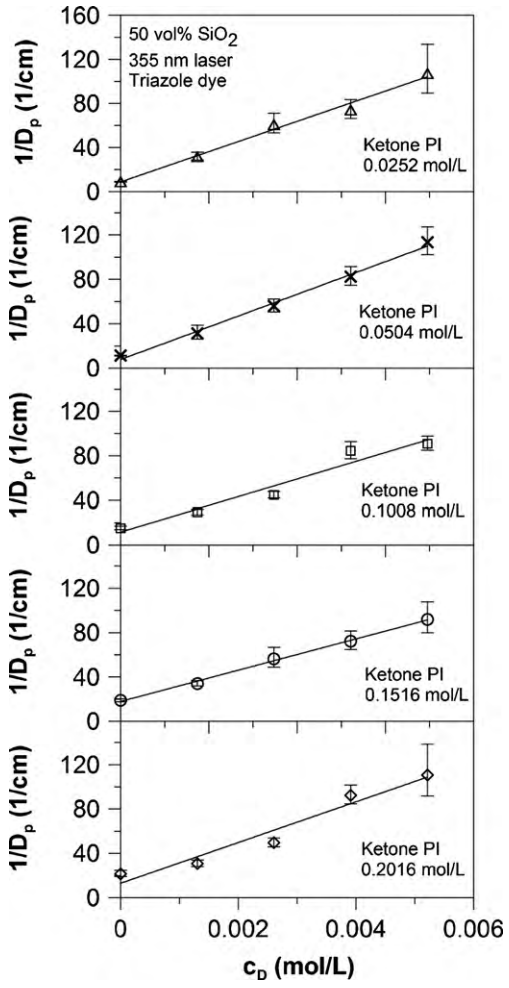

Fig. 7. $1/D_p$ vs. dye concentration c_D for 50 vol% SiO_2 suspensions with ketone PI and triazole dye. Cure depth measurements were performed using the 355 nm laser.

should depend only on volume fraction ceramic and the molar extinction coefficient of the PI. This is approximately the case, and K_4 slopes suggest $\varepsilon_D \sim 26{,}400$ L/(mol cm). The intercepts I_4 from Figs. 7–10 also appear in Table 6a. According to the Absorption Model, Eq. (4b), the slopes I_4 should increase with PI concentration, and it does increase approximately linearly with c_P. This provides another estimate of the extinction coefficient of the PI, which is about $\varepsilon_P \sim 160$ L/(mol cm), which is about the same as the values inferred from the other series of experiments in Fig. 3 and Table 4. The values of I_4 extrapolated to $c_P = 0$ gives another estimate of the scattering term S, which is $\sim 8.3\ cm^{-1}$ for the 50% silica suspensions and $\sim 8.7\ cm^{-1}$ for the 60% silica suspensions, similar to what was inferred from Fig. 3.

Fig. 10 also shows $1/D_p$ vs. dye concentration for a 60 vol% silica suspension with phosphine oxide PI and a blue light absorber, cured with the mercury vapor lamp. In this case the average molar extinction coefficient of the blue light absorber was determined to be $\varepsilon_{D,blue} \sim 2300$ L/(mol cm). The molar extinction coefficient for the blue light measured via spectrophotometry was significantly higher $\sim 13{,}100$ L/(mol cm).

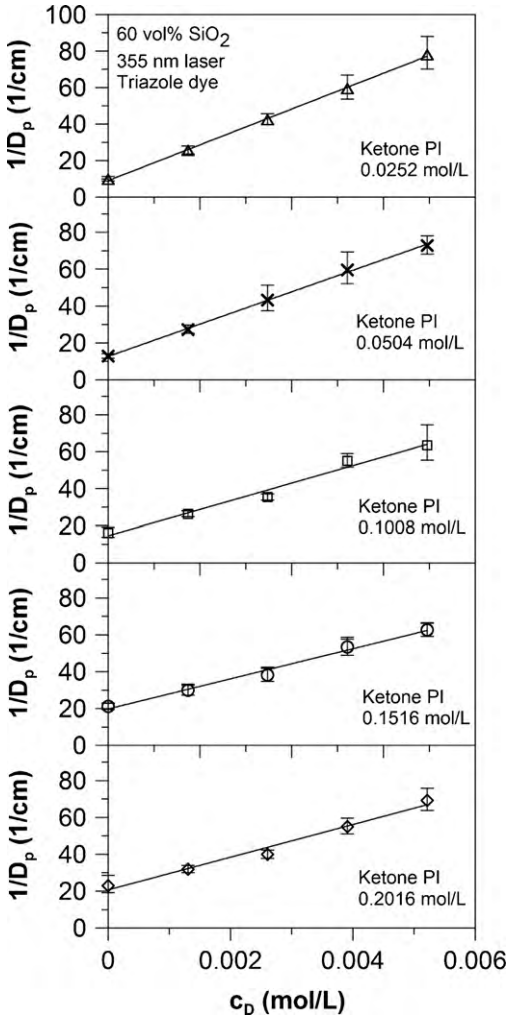

Fig. 8. $1/D_p$ vs. dye concentration c_D for 60 vol% SiO_2 suspensions with ketone PI and triazole dye. Cure depth measurements were performed using the 355 nm laser.

Fig. 10 shows $1/D_p$ vs. c_D plots for alumina suspensions with ketone PI and triazole dye. The slopes, intercepts and correlation coefficients appear in Table 6b. From the alumina suspensions, the molar extinction coefficient of the triazole dye was estimated to be 221,500 L/(mol cm), which is significantly higher than those estimated from the silica suspensions and via spectrophotometry. Similarly to Al_2O_3 suspensions with no dye, one would expect that the D_p should be predominantly determined by the ceramic scattering length and the effect of dye should be negligible, thus resulting in much less steep slope and smaller molar extinction coefficients. Nevertheless, the real observations show that the presence of the triazole dye affects the D_p more than expected.

The values of the extinction coefficients inferred from the cure depth using the Absorption Model are all larger than those measured by spectrophotometry. The phenomena differ, because there is only a small amount of attenuation in the spectrophotometry, while the cure depth measurements, the energy of the UV is attenuated by a factor of 10–20 (as the energy dose changes from E_o at the surface to E_c at a depth of C_d). Spectrophotometry is a low-attenuation measurement, while cure depth is a

Table 6b
Slopes, intercepts and correlation coefficients of linear regressions $1/D_p$ vs. c_D for 55 vol% Al_2O_3 suspensions with ketone PI and triazole dye and for 60 vol% SiO_2 suspensions with phosphine oxide PI and blue light absorber.

Light source	Ceramic	ϕ	PI	c_P [mol/L]	Dye	r^2	K_4	I_4	ε_D [L/(mol cm)]	ε_P [L/(mol cm)]
355 nm laser	Al_2O_3	0.55	Ketone	0.0252	Triazole dye	0.95	123,000 ± 32,000	108.7 ± 21.1	272,000 ± 71,000	2900 ± 600
		0.55	Ketone	0.0504		0.99	77,000 ± 27,000	109.5 ± 20.7	171,000 ± 61,000	1500 ± 300
Average									221,500	2200
Mercury vapor lamp	SiO_2	0.6	Phosphine oxide	0.09844	Blue light absorber	0.92	917 ± 164	20.6 ± 3.2	2300 ± 400	370 ± 60

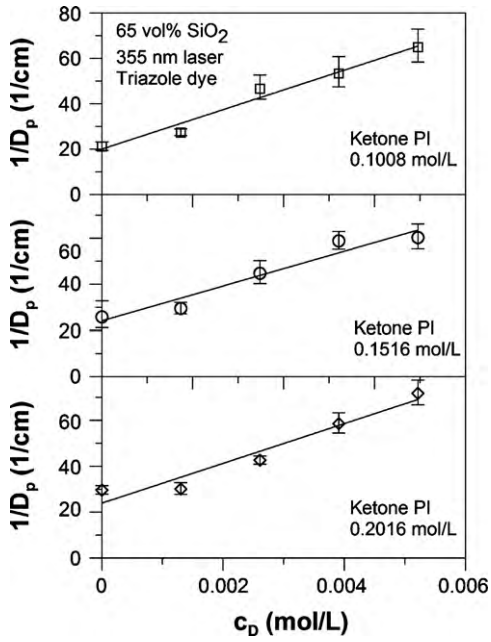

Fig. 9. $1/D_p$ vs. dye concentration c_D for 65 vol% SiO_2 suspensions with ketone PI and triazole dye. Cure depth measurements were performed using the 355 nm laser.

large-attenuation measurement. We might not expect the extinction coefficients to be the same. The Absorption Model assumes the attenuation processes (scattering, dye absorption, PI absorption) are strictly independent. This appears in the derivation of the model (Eq. (6) of reference 5). This assumption leads to the prediction that $1/D_p$ is a linear function of dye and PI concentrations, which is observed. But the magnitude of the extinction coefficients inferred from the slope is too large, as if the model attributes too much attenuation to the PI or dye, so overestimates

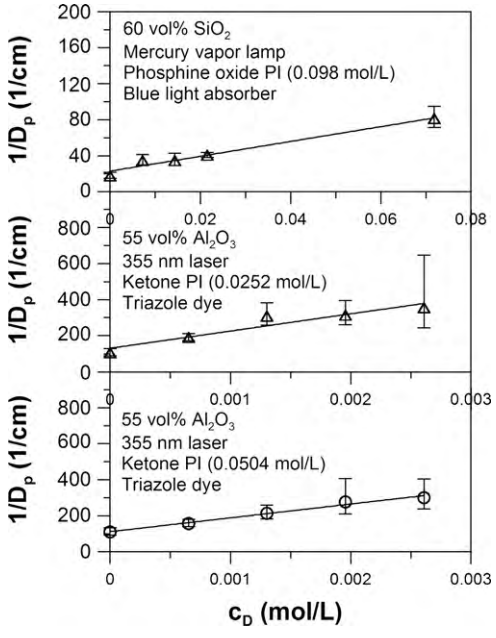

Fig. 10. $1/D_p$ vs. dye concentration c_D for 55 vol% Al_2O_3 suspensions with ketone PI and triazole dye and for 60 vol% SiO_2 suspension with phosphine oxide PI and blue light absorber.

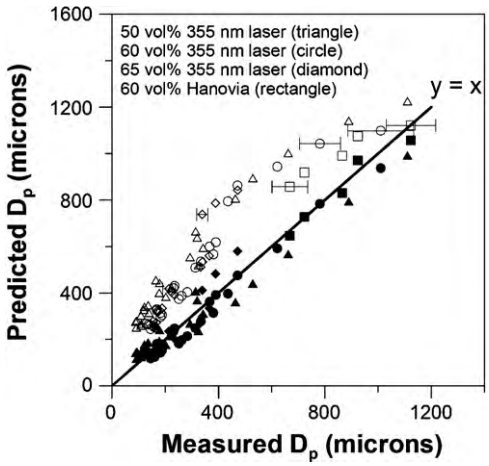

Fig. 11. Predicted vs. measured D_p for 50, 60 and 65 vol% SiO_2 suspensions with varying concentration of ketone photoinitiator and varying amount of UV absorber (triazole dye). Measured data were obtained from cure depth measurements with a 355 nm laser or with the mercury vapor lamp. The error bars are shown for a few points. The predicted data calculated with the Absorption Model with Eq. (2). Closed symbols use extinction coefficients inferred from cure depth measurements in Table 7, open symbols use extinction coefficients from spectrophotometry.

the extinction coefficient. For cases where the ketone PI is not the strongest attenuator, the overestimate of ε_P is much larger. For the alumina suspensions, which are dominated by scattering, the apparent ε_P of the ketone PI is grossly overestimated (Table 4), and in the presence of the strongly absorbing triazole dye, the dependence of $1/D_p$ on c_P does not provide a meaningful value for ε_P.

3.5. Predicted D_p vs. observed D_p

The sensitivity D_p can be calculated from Eq. (2), the Absorption Model, when the scattering term S and the molar extinction coefficients are known. The scattering terms for individual compositions appear in Table 4. The molar extinction coefficients can be measured either via spectrophotometry (Tables 2 and 3) or derived from the Absorption Model as summarized in Table 7. For the predictions, we used the average values of the molar extinction coefficients. Fig. 11 shows the D_p predicted vs. D_p measured for ~70 suspensions with 50, 60 and 65 vol% SiO_2 and varying concentration of ketone photoinitiator and varying amount of triazole dye UV absorber. The measured data were obtained from cure depth measurements with a 355 nm laser or with the mercury vapor lamp. Error bars for the measured D_p are shown for only few points, to avoid cluttering the graph. These are typical measurement error bars. The closed symbols have the predicted D_p calculated from Eq. (2) using the S parameters from Table 4 and the average extinction coefficients inferred from cure depth measurements in Table 7, which were $\varepsilon_P = 200$ L/(mol cm) for the ketone PI and $\varepsilon_D = 29{,}900$ L/(mol cm) for the triazole dye. Using these two extinction coefficients, the D_p of more than 50 different compositions of photopolymerizable suspensions, ranging from ~100 to ~1000 μm, can be calculated within the accuracy of the measurement, as indicated by the typical error bars. The open symbols have the predicted D_p using extinc-

Table 7
Molar absorption coefficients of the PIs and dyes derived from the model.

	Plot $1/D_p$ vs.	Eq.	Light source	Suspensions	PI	Dye	L/(mol cm)
ε_P	c_P	K_3	355 nm laser	SiO_2	Ketone	Triazole dye	220
	c_D	I_4					180
Average used in Fig. 11							200
ε_P	c_P	K_3	355 nm laser	Al_2O_3	Ketone	Triazole dye	1600
	c_D	I_4					2200
Average							1900
ε_D	c_P	I_3	355 nm laser	SiO_2	Ketone	Triazole dye	33,400
	c_D	K_4					26,400
Average used in Fig. 11							29,900
ε_P	c_P	K_3	Mercury vapor lamp	SiO_2	Ketone	–	80
ε_P	c_P	K_3	Mercury vapor lamp	SiO_2	Phosphine oxide	–	210
ε_D	c_D	K_4	Mercury vapor lamp	SiO_2	Phosphine oxide	Blue light absorber	2300
ε_D	c_D	K_4	355 nm laser	Al_2O_3	Ketone	Triazole dye	221,500

tion coefficients measured by spectrophotometry and listed in Table 3. As the extinction coefficients from spectroscopy are smaller than those derived from the cure depth measurements, the D_p values predicted with them significantly overestimate the measured D_p, sometimes as much as a factor of two. Considering the wide spectra of compositions prepared with varying PIs and dyes concentration, varying ceramic volume content and using either the 355 nm laser or mercury vapor lamp with multiple lines, the predicted and measured values provide a satisfactory match.

4. Conclusions

The compositional dependence of the sensitivity parameter D_p, which relates cure depth C_d to energy dose E for UV photopolymerizable ceramic suspensions, can be accurately modeled in terms of the attenuation of the UV radiation by absorption of the photoinitiator, inert dyes, and scattering by the ceramic particles.

This Absorption Model predicts that the inverse of the sensitivity parameter, $1/D_p$, should be a linear function of photoinitiator concentration. This is observed, and a self-consistent value for the photoinitiator extinction coefficient derived from the slope agrees with a wide range of compositions. The extinction coefficients derived from the Absorption Model from cure depth measurements in acrylate monomers are larger than extinction coefficients measured by spectrophotometry in dilute isopropanol solution.

The model predicts that the slope should be proportional to the ceramic volume fraction, and this agrees with measured data.

The model predicts that $1/D_p$, should be a linear function of dye concentration. This is observed, and a self-consistent value for the dye extinction coefficient derived from the slope agrees with a wide range of compositions. The dye extinction coefficients derived from the Absorption Model from cure depth measurements in acrylate monomers are larger than dye extinction coefficients measured by spectrophotometry in dilute isopropanol solution.

Scattering lengths inferred from the Absorption Model are in the correct range for silica and alumina suspensions.

Using extinction coefficients derived from cure depth measurements, the compositional dependence for the predicted values for sensitivity D_p agrees with measured values within measurement error. Using extinction coefficients derived from spectrophotometry, the compositional dependences for the predicted values for sensitivity D_p are overestimated.

Acknowledgements

This research was supported by the United States Defense Advanced Research Projects Agency (DARPA) under HR0011-07-1-0034, Program Officer W.S. Coblenz and the Office of Naval Research under N00421-06-1-002, Program Officer David Shifler.

References

1. Stansbury JW. Curing dental resins and composties by photopolymerization. *J Esteht Dent* 2000;**12**(6):300–8.
2. Lee HD, Pober RL, Calvert PD, Bowen HK. Photopolymerizable binders for ceramics. *J Mater Sci Lett* 1986;**5**:81–181.
3. De Hazan Y, Heinecke J, Weber A, Graule T. High solids loading ceramic colloidal dispersions in UV curable media with via comb-polyelectrolyte dispersants. *J Colloid Interface Sci* September 2009;**337**(1):66–74.
4. Halloran JW, Bae C-J, Torres-Garibay C, Tomeckova V, Das S, Baker W. Manufacture of complex ceramics by photopolymerization. In: Alida Bellosi, Nicola Babini G, editors. *The Proceedings of the 2nd International Congress on Ceramics, Global Roadmap for Ceramics-ICC2 Proceedings*. Faenza, Italy: Agenzia Polo Ceramico S.C. A.r.l.; 2008. p. 369–78. ISBN:978-88-8080-084-2.
5. Jacobs PF. Rapid prototyping & manufacturing—fundamentals of stereolithography. *Soc Manuf Eng* 1992.
6. Tomeckova, V., Halloran, J. W., Predictive models for the photopolymerization of ceramic suspensions. *J Eur Ceram Soc*, JECS 7799, in press, online available February 2010.
7. Tomeckova, V., Halloran, J. W., Critical energy for photopolymerization of ceramic suspensions. *J Eur Ceram Soc*, (17) March, in press, June 2010.
8. Griffith ML, Halloran JW. Scattering of ultraviolet radiation in turbid ceramic suspensions. *J Appl Phys* 1997;**81**(10):2538–46.

9. Abouliatim Y, Chartier T, Abelard P, Chaput C, Delage D. Optical characterization of stereolithography suspensions using the Kubelka–Munk model. *J Eur Ceram Soc* 2009;**29**(5):919–24.
10. Wu KC, Seefeldt KF, Solomon MJ, Halloran JW. Prediction of ceramic stereolithography resin sensitivity from theory and measurement of diffusive photon transport. *J Appl Phys* July 2005;**98**(15):024902-1–124902-10.
11. Garg R, Prud'homme R, Aksay I, Liu, Alfano R. Adsorption length for photo propagation in highly dense colloidal dispersions. *J Mater Sci* 1998;**13**(12):3463–7.